**Article:**
Wang, K, Tan, W, Si, Y et al. (3 more authors) (2024) A solute transport in deformable dual-porosity media using mixture-coupling theory. Environmental Geotechnics, 11 (3). pp. 165-179. ISSN 2051-803X

https://doi.org/10.1680/jenge.22.00029

# A Mixture Coupling Theory based model for solute transport in deformable dual-porosity media

**Kai Wang[1]; Wenjie Tan[2]; Yanxiao Si[2]; Yue Ma[3]; Xiao-Hui Chen[3]; Aizhong Ding[1*]**

[1]College of Water Sciences, Beijing Normal University, Beijing, 100875, CHINA

[2]Surface engineering division, Sinopec Petroleum exploration and production research institute, Beijing, 102206, CHINA

[3]School of Civil Engineering, University of Leeds, Leeds, LS2 9JT, UK

[*] Corresponding author: Aizhong Ding. E-mail address: ading@bnu.edu.cn

Submitted: 28 February 2022

Number of words in the main text: 4999

Number of figures and tables: 9 figures and 3 tables

**Abstract**

Rock, soil and many porous-like materials are often fractured or structured media, which can exhibit dual-porosity behaviour. Studies on solute transport in deformable dual-porosity media remain challenging due to the multi-physics coupled effects and the complex interaction between fracture (or macropore) and porous matrix. Though several studies exist on constitutive modelling of coupled behaviour in deformable dual-porosity, the previously developed models are not systematic in thermodynamical frameworks. This paper proposes a Mixture Coupling Theory approach based on nonequilibrium thermodynamics to develop the solute transport model with consideration of hydro-mechanical coupling in dual-porosity media (referred to as the ST-HM model). This paper derives the constitutive equations of fully hydro-mechanical coupled behaviour in dual-porosity media and considers the pore and fracture porosity evolution influenced by both hydro and mechanical fields. Therefore, the governing equations of ST-HM are capable of predicting non-reactive solute transport with a fully hydro-mechanical coupled effect in dual-porosity media. Then, the model was verified against existing models and validated by relevant experimental results. Further, a numerical example shows that the presented model significantly improves the accuracy of the prediction of porosity, fluid pressure, and solute concentration compared with previous models, which ignore the fully hydro-mechanical coupled effects on solute transport.

**Keywords:** Solute transport; Deformable dual-porosity media; Coupled model; Nonequilibrium thermodynamics; Mixture Coupling Theory

**List of notations**

$B$ material coefficient

$c_{\alpha c}$ solute mass fraction

$C$ solute volumetric concentration

$\mathbf{d}$ displacement vector

$d_i$ displacement in $i$ axis

$D^{\alpha}$ dispersion - diffusion coefficient for solute

$\mathbf{E}$ Green strain

$\mathbf{F}$ deformation gradient

$G$ shear modulus

$H_{ij}$ material-dependent parameter

$\mathbf{I}^{\alpha\beta}$ mass flux

$J$ Jacobian of $\mathbf{F}$

$\mathbf{J}^{\alpha\beta}$ diffusion flux

$k_0^{\alpha}$ initial permeability

$k^{\alpha}$ permeability

$K$ bulk modulus of total geomaterial

$K_s$ bulk modulus of solid grain

$K_w$ bulk modulus of water

$K_{pb}$ bulk modulus of the porous matrix block

$L$ fracture spacing

$L_{ijkl}$ material-dependent parameter

$m^{\alpha\beta}$ mass density in the reference configuration

$M_{ij}$ material-dependent parameter

$\mathbf{n}$ outward unit normal vector

$N$ dimension of porous matrix block ( $N$ =1,2,3)

$p^{\alpha l}$ fluid pressure

$Q$ material coefficient

$r_{ex}^{\beta}$ exchange flux between the pore and fracture

$S_{ij}$ material-dependent parameter

$S$ boundary of an arbitrary region

$t$ Time

$\mathbf{T}$ second Piola-Kirchhoff stress

$T$ temperature.

$\upsilon^{\alpha}$ porosity in the reference configuration

$\upsilon_0^{\alpha}$ initial porosity in the reference configuration

$\mathbf{u}^{\alpha l}$ Darcy velocity of fluid

$\nu$ Poisson's ratio

$\mathbf{v}_s$ velocity of a solid.

$V$ an arbitrary region in the current configuration

$V_0$ an arbitrary region in the reference configuration

$W$ deformation energy (dual potential)

$\mathbf{x}$ material point for one phase in an arbitrary current configuration

$\mathbf{X}$ material point for one phase in an arbitrary reference configuration

$Z$ material coefficients

**Greek symbols**

$\gamma$ entropy production per unit volume

$\varepsilon_{ij}$ strain tensor

$\zeta^{\alpha}$ Biot constant

$\mu_w$ dynamic viscosity of water

$\mu^{\alpha\beta}$ chemical potential

$\nabla\mu_{ex}^{\beta}$ gradient of the chemical potential of exchange water or solute

$\rho^{\alpha\beta}$ mixture density

$\rho_l^{\alpha\beta}$ In-phase density (true density)

$\boldsymbol{\sigma}$ Cauchy stress

$\phi^{\alpha}$ porosity in current configuration

$\phi^{S}$ volume fraction of the solid part

$\psi$ Helmholtz free energy density

$\psi_{\alpha}$ Helmholtz free energy density of the bulk fluid

$\chi$ shape factor

$\tau$ diffusion transfer parameter

$\Psi$ Helmholtz free energy density in the reference configuration

$\vartheta_{\alpha l}$ entropy production of fluid flow

$\vartheta_{ex}$ entropy production of fluid exchange between pore and fracture

**Subscripts and superscripts**

$\alpha = M$ For pore

$\alpha = F$ For fracture

$\beta = w$ For water

$\beta = c$ For solute

$\beta = l$ For liquid (solution)

## Introduction

Rock, soil, and many porous-like materials are fractured or structured in reality and exhibit very different characteristics than ideal porous media (Duguid and Lee, 1977, Berre et al., 2019). For fractured and structured porous media, which contains both macropores and porous matrix, the most distinctive properties compared to single porosity media are the very heterogeneous distribution of porosity, permeability, and the interaction between fracture (or macropore) and porous matrix. Here, fractured porous media represents both fractured and structured media. Understanding the fluid flow and solute transport in fractured porous media is very important in groundwater remediation, agriculture engineering, and underground construction (Rutqvist and Stephansson, 2003, Molson et al., 2012, Ray, 1994). Also, the exploitation of naturally fractured reservoirs needs to study the fluid and solute flow in the fractured rock (Liu et al., 2019, Savatorova et al., 2016). Geological carbon storage (GCS) technology often experiences chemo-hydro-mechanical coupled processes in fractured rocks during carbon sequestration (Akono et al., 2019).

So far, several methods have been considered to study the fluid and solute transport in fractured porous media, including laboratory experiments (Leij et al., 2012), numerical studies (Kodešova et al., 2006) and mathematical models (Berre et al., 2019). In the previous studies, continuum models (Shu, 1999, Li et al., 2020, Saevik et al., 2013, Dykhuizen, 1990) were used, this includes research on permeability tensor by Oda (Oda, 1985), one of the earliest studies, and other damage mechanics studies in fractured

media (De Bellis et al., 2017, De Bellis et al., 2016, Arson and Pereira, 2013). Also, many researchers used discrete fracture models (Lee et al., 2001, Jiang and Younis, 2017) to represent fractured porous media. The dual-porosity model (also called the double porosity model), one of the multi-continuum models, was firstly presented by Barenblatt in 1960 s (Barenblatt et al., 1960). This theory assumes that fractured porous media can be viewed as two overlapping domains, porous matrix and fracture (shown in **Figure 1**); they are both continua but with different characteristics such as permeability, porosity, bulk modulus and so on. In addition, the water and solute exchange happens between fracture and porous matrix. However, the dual-porosity model cannot present a geometric distinction between porous matrix and fracture, as it employs a continuum to simplify the fracture network.

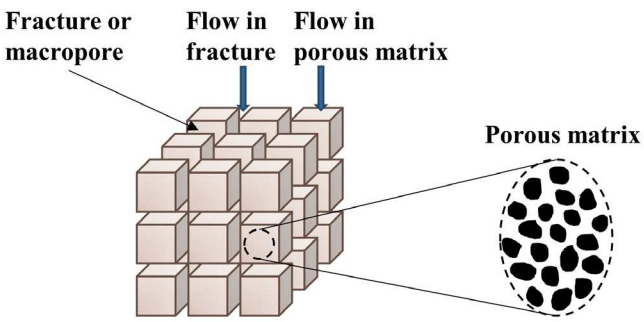


**Figure 1.** Conceptual description of the dual-porosity theory

A more realistic understanding of solute transport needs a further understanding of the coupled model because, natural rocks always exist in a multi-physics coupled environment. Biot (Biot, 1941) and Terzaghi (Terzaghi, 1943) are the pioneers of hydro-mechanical coupled consolidation theory. Based on these theories, Khalili et al. studied the Hydro-Mechanical and Thermo-Hydro-Mechanical coupling in deformable dual-

porosity media (Khalili, 2003, Gelet et al., 2012b, Khalili, 2008a). In addition, several solute transport models (Murad and Moyne, 2008, Revil, 2017) and Hydro-Mechanical-Chemical coupled models (Li et al., 2020, Musso et al., 2013, Vecchia and Musso, 2016) in dual-porosity media were developed recently. However, these studies often ignore the fully hydro-mechanical coupling (especially the porosity evolution induced by fluid pressure), which may strongly influence solute transport. These models can be termed as mechanics approach (most widely used by researchers since Terzhagi developed 1D consolidation theory) models as their derivation is mainly based on mechanics and momentum balance. Mechanics approach can easily develop new coupled models in by introducing equations from other disciplines (e.g. adding chemical reaction equations into solute transport equation), while lacking a systemic framework that covers different fields (Chen et al., 2016).

On the other hand, the Mixture Theory, which adopts a different approach, was developed from the study of biological tissues at the early stage (Bowen, 1976) but, gained more and more attention from geological and environmental researchers in recent years. In the Mixture Theory, each point in the mixture is assumed to contain every component (for example, solid and fluid) (Bedford and Drumheller, 1983). Several works have been carried out on coupled fluid transport and porous media deformation (Drumheller, 1978, Bowen, 1984, Rajagopal and K., 2007, Hutter et al., 2015).

Mixture Coupling Theory (originally named Modified Mixture Theory) is an emerging

approach developed by Heidug and Wong (Heidug and Wong, 1996). This theory is based on nonequilibrium thermodynamics and Mixture Theory, which makes it a energy-based theory. Mixture Coupling Theory has been used to derive the Hydro-Mechanical model (Chen and Hicks, 2011, Chen, 2013), Hydro-Mechanical-Chemical and Thermo-Hydro-Mechanical-Chemical model (Chen and Hicks, 2013, Ma et al., 2021) in porous media. The Mixture Coupling Theory links different physical fields using Helmholtz free energy and obtains the coupling relationships of stress, porosity and other variables by deformation energy analysis.

Mixture theory uses the internal frictional interaction force to study information on the interaction between different components, which is hard to obtain (Laloui et al., 2003). In comparison, Mixture Coupling Theory uses entropy production to study the interaction between each component, which makes it easier to consider molecule-scale friction or other chemical-induced dissipative processes.

The presented paper used the Mixture Coupling Theory to derive a systematic solute transport model with consideration of hydro-mechanical coupling in dual-porosity media (referred to as the ST-HM model) based on nonequilibrium thermodynamics. This model successfully determines the non-reactive solute transport behaviour with fully hydro-mechanical coupling effects, and considers porosity and permeability evolution influenced by solid deformation, porous/fracture fluid pressure, and the coupled interaction between porous and fracture fluid flow. The new model is compared with previous models derived by the mechanics approach and validated against

experimental data. A numerical simulation is further performed to investigate the potential application of the proposed model in groundwater contamination research.

## Constitutive equation development

*Balance equation of Helmholtz free energy and entropy production*

An arbitrary region $V$ with a boundary $S$ is selected for this to study the dual-porosity medium. Water and solute fluxes can pass through the boundary while the solid phase cannot; and only one solute is considered in this study. The local version balance equation of Helmholtz free energy for the open system can be obtained in a dual-porosity media as

$$\dot{\psi} + \psi \nabla \cdot \mathbf{v}^s - \nabla \cdot (\boldsymbol{\sigma} \mathbf{v}^s) + \nabla \cdot (\mu^{Mw} \mathbf{I}^{Mw} + \mu^{Mc} \mathbf{I}^{Mc}) + \nabla \cdot (\mu^{Fw} \mathbf{I}^{Fw} + \mu^{Fc} \mathbf{I}^{Fc}) = -T\gamma \leq 0 \tag{1}$$

where $\psi$ is the Helmholtz free energy density, $\boldsymbol{\sigma}$ is the Cauchy stress tensor, $\mathbf{v}^s$ is the velocity of a solid, $\mu^{Mw}$, $\mu^{Fw}$, $\mu^{Mc}$, $\mu^{Fc}$ are the chemical potential of pore water, fracture water, solute in porous flow, solute in fracture flow, respectively. $\mathbf{I}^{Mw}$, $\mathbf{I}^{Mc}$, $\mathbf{I}^{Fw}$, $\mathbf{I}^{Fc}$ are the flux of pore water, porous solute, fracture water, and fracture solute, respectively. $T$ is the constant temperature and $\gamma$ is the entropy production per unit volume.

The detailed derivation of equation (1) is presented in Supplementary information.

It is assumed that only the friction generated at the solid-fluid (water and solute) interface contributes to the energy dissipation in the mixture. By using the equation of entropy production of water and solute flow (Katachalsky and Curran, 1965) and the equation for fluid exchange between porous and fracture space (Gelet et al., 2012b,

Coussy, 2004), the entropy production of the dual-porosity media can be obtained as

$$0 \le T\gamma = -\mathbf{I}^{Mw} \cdot \nabla \mu^{Mw} - \mathbf{I}^{Mc} \cdot \nabla \mu^{Mc} - \mathbf{I}^{Fw} \cdot \nabla \mu^{Fw} - \mathbf{I}^{Fc} \cdot \nabla \mu^{Fc} + r_{ex}^{w}\left(\mu^{Mw} - \mu^{Fw}\right) + r_{ex}^{c}\left(\mu^{Mc} - \mu^{Fc}\right) \tag{2}$$

where $r_{ex}^{w}$ and $r_{ex}^{c}$ are the exchange water and solute flux between the pore and fracture. The chemical potential of exchange water changes from $\mu^{Mw}$ to $\mu^{Fw}$ when the exchange is to fracture, from $\mu^{Fw}$ to $\mu^{Mw}$ vice versa.

*Basic equations of water and solute flow in dual-porosity media*

In this manuscript, both mixture density and In-phase (also called true density) density are used. The mixture density can be obtained by the In-phase density of pore water $\rho_l^{Mw}$, fracture water $\rho_l^{Fw}$, porous solute $\rho_l^{Mc}$ and fracture solute $\rho_l^{Fc}$ as

$$\rho^{Mw} = \phi^{M}\rho_l^{Mw}, \rho^{Fw} = \phi^{F}\rho_l^{Fw}, \rho^{Mc} = \phi^{M}\rho_l^{Mc}, \rho^{Fc} = \phi^{F}\rho_l^{Fc} \tag{3}$$

where $\phi^{M}$, $\phi^{F}$ are the porosity of porous matrix and fracture, and they obey

$$\phi^{M} + \phi^{F} + \phi^{S} = 1 \tag{4}$$

where $\phi^{S}$ is the volume fraction of the solid phase.

In-phase density refers to the mass of a specified component per unit phase volume (for example, the mass of solute per unit liquid volume). Here, using In-phase density instead of true density avoids confusion since true density can easily be misunderstood with the intrinsic density of one component, such as solid salt.

The In-phase density of the solution in the porous matrix and fracture is defined as

$$\rho_l^{Ml} = \rho_l^{Mc} + \rho_l^{Mw}, \rho_l^{Fl} = \rho_l^{Fc} + \rho_l^{Fc} \tag{5}$$

The balance equation of fluid writes

$$(\upsilon^M \rho_l^{Ml})^{\cdot} + \nabla \cdot (\rho_l^{Ml} \mathbf{u}^{Ml}) + r_{ex}^l = 0 \tag{6}$$

$$(\upsilon^F \rho_l^{Fl})^{\cdot} + \nabla \cdot (\rho_l^{Fl} \mathbf{u}^{Fl}) - r_{ex}^l = 0 \tag{7}$$

where $\upsilon^M = J\phi^M$ and $\upsilon^F = J\phi^F$ are pore volume per unit referential volume and fracture volume per unit referential volume, and $r_{ex}^l = r_{ex}^w + r_{ex}^c$ is the fluid mass exchange between pore and fracture, $\mathbf{u}^{Ml}$ and $\mathbf{u}^{Fl}$ are the Darcy velocity of the porous fluid and fracture fluid, $J$ is the Jacobian of the deformation gradient $\mathbf{F}$.

Also, the balance equation of solute in porous matrix and fracture can be derived as

$$(\upsilon^M \rho_l^{Ml})\dot{c}_{Mc} + \rho_l^{Ml} \mathbf{u}^{Ml} \nabla c_{Mc} + r_{ex}^c + \nabla \cdot \mathbf{J}^{Mc} = 0 \tag{8}$$

$$(\upsilon^F \rho_l^{Fl})\dot{c}_{Fc} + \rho_l^{Fl} \mathbf{u}^{Fl} \nabla c_{Fc} - r_{ex}^c + \nabla \cdot \mathbf{J}^{Fc} = 0 \tag{9}$$

where $c_{Mc} = \dfrac{\rho_l^{Mc}}{\rho_l^{Ml}}$, $c_{Fc} = \dfrac{\rho_l^{Fc}}{\rho_l^{Fl}}$ are the solute mass fraction, $\mathbf{J}^{Mc}$, and $\mathbf{J}^{Fc}$ are the diffusion flux of porous solute and fracture solute.

The detailed derivation of the balance equation is presented in Supplementary information.

*Basic equation of state*

Based on the assumption that the dual-porosity media maintain mechanical equilibrium and without volume force, so $\nabla \cdot \boldsymbol{\sigma} = \mathbf{0}$. By using equation (1) and (2), it leads to

$$\dot{\psi} + \psi \nabla \cdot \mathbf{v}^s - \nabla \cdot (\boldsymbol{\sigma} \mathbf{v}^s) + (\mu^{Mw} \nabla \cdot \mathbf{I}^{Mw} + \mu^{Mc} \nabla \cdot \mathbf{I}^{Mc}) + (\mu^{Fw} \nabla \cdot \mathbf{I}^{Fw} + \mu^{Fc} \nabla \cdot \mathbf{I}^{Fc}) + r_{ex}^w \left(\mu^{Mw} - \mu^{Fw}\right) + r_{ex}^w \left(\mu^{Mc} - \mu^{Fc}\right) = 0 \tag{10}$$

Based on the mass balance equation and using equation (10), using finite strain theory in continuum mechanics, the free energy in the reference configuration can be obtained as

$$\dot{\Psi} = tr(\mathbf{T}\dot{\mathbf{E}}) + \mu^{Mw}\dot{m}^{Mw} + \mu^{Fw}\dot{m}^{Fw} + \mu^{Mc}\dot{m}^{Mc} + \mu^{Fc}\dot{m}^{Fc} \tag{11}$$

where $\Psi = J\psi$, $\mathbf{E}$ represents Green strain, $\mathbf{T}$ is the second Piola-Kirchhoff stress, $m^{Mw} = J\rho^{Mw}$, $m^{Fw} = J\rho^{Fw}$, $m^{Mc} = J\rho^{Mc}$, $m^{Fc} = J\rho^{Fc}$ are the mass density of pore water, fracture water, porous solute, and fracture solute in the reference configuration. The detailed derivation of equation (11) is presented in Supplementary information.

*Helmholtz free energy density of the fluid and solid skeleton*

The derivation of the Helmholtz free energy density of the bulk fluid in porous matrix and fracture requires some of the following assumptions to be made. The fluid flow is isothermal, the equilibrium is transient (i.e. porosity can be viewed as a constant), and the chemical is non-reactive. The fluid is non-sorptive, and this is necessitated as Brochard and Honório points out that the Gibbs-Duhem equation does not hold well, in general, for an adsorbed fluid (Brochard and Honório, 2020). Based on the above assumptions, water/fluid in the pores and fractures is not strongly influenced by intermolecular and surface forces. So the Helmholtz free energy density of the bulk fluid in porous matrix and fracture can be derived as

$$\psi_M = -p^{Ml} + \left(\mu^{Mw}\rho_l^{Mw} + \mu^{Mc}\rho_l^{Mc}\right) \tag{12}$$

$$\psi_F = -p^{Fl} + \left(\mu^{Fw}\rho_l^{Fw} + \mu^{Fc}\rho_l^{Fc}\right) \tag{13}$$

where $p^{Ml}$ is the porous fluid pressure and $p^{Fl}$ is the fracture fluid pressure. Using Gibbs–Duhem equation, there are

$$\dot{\psi}_M = \dot{\rho}_l^{Mw}\mu^{Mw} + \dot{\rho}_l^{Mc}\mu^{Mc} \tag{14}$$

$$\dot{\psi}_F = \dot{\rho}_l^{Fw}\mu^{Fw} + \dot{\rho}_l^{Fc}\mu^{Fc} \tag{15}$$

Using equation (11), (12), (13), (14), (15) and equation (3), the free energy of the solid skeleton (including solid phase and water molecules attached to the solid's surface) can be described as:

$$\left(\Psi - J\phi^M\psi_M - J\phi^F\psi_F\right)^{\cdot} = tr(\mathbf{T}\dot{\mathbf{E}}) + \dot{\upsilon}^M p^{Ml} + \dot{\upsilon}^F p^{Fl} \tag{16}$$

*Constitutive equations*

Subtracting the contribution of porous fluid pressure and fracture fluid pressure from Helmholtz free energy density of the solid skeleton, the deformation energy (also called dual potential) can be obtained

$$W = \left(\Psi - J\phi^M\psi_M - J\phi^F\psi_F\right) - \upsilon^M p^{Ml} - \upsilon^F p^{Fl} \tag{17}$$

The time derivative of deformation energy can be obtained using equation (16) and (17) as

$$\dot{W} = tr(\mathbf{T}\dot{\mathbf{E}}) - \upsilon^M \dot{p}^{Ml} - \upsilon^F \dot{p}^{Fl} \tag{18}$$

Equation (18) shows that $W$ is a function of $\mathbf{E}$, $p^{Ml}$ and $p^{Fl}$.

From equation (18), the expression of $\mathbf{T}$, $\upsilon^M$ and $\upsilon^F$ can be obtained as

$$T_{ij} = \left(\frac{\partial W}{\partial E_{ij}}\right)_{p^{Ml},p^{Fl}}, \upsilon^M = -\left(\frac{\partial W}{\partial p^{Ml}}\right)_{E_{ij},p^{Fl}}, \upsilon^F = -\left(\frac{\partial W}{\partial p^{Fl}}\right)_{E_{ij},p^{Ml}} \tag{19}$$

So that

$$\dot{W}(\mathbf{E}, p^{Ml}, p^{Fl}) = \left(\frac{\partial W}{\partial E_{ij}}\right)_{p^{Ml}, p^{Fl}} \dot{E}_{ij} + \left(\frac{\partial W}{\partial p^{Ml}}\right)_{E_{ij}, p^{Fl}} \dot{p}^{Ml} + \left(\frac{\partial W}{\partial p^{Fl}}\right)_{E_{ij}, p^{Ml}} \dot{p}^{Fl}$$

(20)

By differentiating equation (19), and using equation (20), the basic constitutive equation for the evolution of stress, pore porosity and fracture porosity can be obtained as

$$\dot{T}_{ij} = L_{ijkl}\dot{E}_{kl} - M_{ij}\dot{p}^{Ml} - S_{ij}\dot{p}^{Fl} \tag{21}$$

$$\dot{\upsilon}^{M} = M_{ij}\dot{E}_{ij} + Q\dot{p}^{Ml} + B\dot{p}^{Fl} \tag{22}$$

$$\dot{\upsilon}^{F} = S_{ij}\dot{E}_{ij} + B\dot{p}^{Ml} + Z\dot{p}^{Fl} \tag{23}$$

where the parameters $L_{ijkl}$, $M_{ij}$, $S_{ij}$, $H_{ij}$, $B$, $Q$, $Z$, defined by the following equations

## Coupled field equations

### *Assumptions in dual-porosity media*

Some simplifications and assumptions are made to simplify the further discussion.

1. Small strain condition is adopted in this paper, so the Green Strain tensor $E_{ij}$ and Piola-Kirchhoff stress $T_{ij}$ can be replaced by strain tensor $\varepsilon_{ij}$ and Cauchy stress $\sigma_{ij}$.

2. The parameters $L_{ijkl}$, $M_{ij}$, $S_{ij}$, $Z$, $B$, $Q$ are all material-dependent constants.

3. The rock is assumed to be isotropic, so that

$$M_{ij} = \zeta^{M}\delta_{ij} \quad , \quad S_{ij} = \zeta^{F}\delta_{ij}, \quad L_{ijkl} = G(\delta_{ik}\delta_{jl} + \delta_{il}\delta_{jk}) + (K - \frac{2G}{3})\delta_{ij}\delta_{kl} \tag{24}$$

where $G$ and $K$ are the shear modulus and bulk modulus of the rock.

Similarly, the pore and fracture porosity equation (22) and (23) become

$$\dot{\upsilon}^{M} = \zeta^{M}\dot{\varepsilon}_{ii} + Q\dot{p}^{Ml} + B\dot{p}^{Fl} \tag{25}$$

$$\dot{\upsilon}^{F} = \zeta^{F}\dot{\varepsilon}_{ii} + B\dot{p}^{Ml} + Z\dot{p}^{Fl} \tag{26}$$

The evolution of pore and fracture permeability can be obtained using the Kozeny-Carman function(Bitzer, 1996)

$$k^{M} = k_{0}^{M}\left(\frac{\upsilon^{M}}{\upsilon_{0}^{M}}\right)^{3}\left(\frac{1-\upsilon_{0}^{M}}{1-\upsilon^{M}}\right)^{2} \tag{27}$$

$$k^{F} = k_{0}^{F}\left(\frac{\upsilon^{F}}{\upsilon_{0}^{F}}\right)^{3}\left(\frac{1-\upsilon_{0}^{F}}{1-\upsilon^{F}}\right)^{2} \tag{28}$$

where $k_0^M$ and $k_0^F$ are the initial pore and fracture permeability, $\upsilon_0^M$ and $\upsilon_0^F$ are the initial pore and fracture porosity.

*Multi-physics governing equations of solute transport in dual-porosity media*

Mechanical static equilibrium is assumed here, so $\partial\sigma_{ij}/\partial x_j = 0$, using displacement variables $d_i (i = 1,2,3)$ through $\varepsilon_{ij} = \frac{1}{2}(d_{i,j} + d_{j,i})$ and $\dot{\varepsilon}_{ii} = \nabla\cdot\dot{\mathbf{d}}$, the mechanical governing equation can be described as

$$G\nabla^{2}\dot{\mathbf{d}} + \left(\frac{G}{1-2\nu}\right)\nabla(\nabla\cdot\dot{\mathbf{d}}) - \zeta^{M}\nabla\dot{p}^{Ml} - \zeta^{F}\nabla\dot{p}^{Fl} = 0 \tag{29}$$

where $\nu$ is Poisson's ratio.

If the influence of solute on fluid pressure is neglected, the variation of the In-phase density of the porous fluid is

$$\dot{\rho}_l^{Ml} = \rho_l^{Ml}\left(\frac{1}{\rho_l^{Ml}}\frac{\partial \rho_l^{Ml}}{\partial p^{Ml}}\right)\frac{\partial p^{Ml}}{\partial t} = \rho_l^{Ml}\frac{1}{K_w}\dot{p}^{Ml} \tag{30}$$

where $K_w$ is the bulk modulus of water.

Using the pore porosity equation (25), Darcy's law, and displacement $\mathbf{d}$, substituting equation (30) into equation (6), the balance equation of porous fluid (equation (6))becomes

$$\zeta^M \nabla \cdot \dot{\mathbf{d}} + (Q + \upsilon^M \frac{1}{K_w})\dot{p}^{Ml} + B\dot{p}^{Fl} + \frac{r_{ex}^l}{\rho_l^{Ml}} - \frac{k^M}{\mu_w}\nabla^2 p^{Ml} = 0 \tag{31}$$

where $k^M$ is the permeability for the porous matrix, $\mu_w$ the water dynamic viscosity (normally related to water temperature), $p^{Ml}$ the fluid pressure in the porous matrix.

Similar to the above steps of porous fluid, the governing equation for fracture fluid transport can be obtained as

$$\zeta^F \nabla \cdot \dot{\mathbf{d}} + (Z + \upsilon^F \frac{1}{K_w})\dot{p}^{Fl} + B\dot{p}^{Ml} - \frac{r_{ex}^l}{\rho_l^{Fl}} - \frac{k^F}{\mu_w}\nabla^2 p^{Fl} = 0 \tag{32}$$

where $k^F$ is the permeability for fracture, $p^{Fl}$ is the fluid pressure in fracture.

Using Darcy's law and Fick's law in the balance equation of porous solute transport, the governing equation for porous solute transport is

$$(\upsilon^M \rho_l^{Ml})\dot{c}_{Mc} - \rho_l^{Ml}\frac{k^M}{\mu_w}\nabla p^{Ml}\nabla c_{Mc} + r_{ex}^c + \nabla \cdot (\rho_l^{Ml} D^M \nabla c_{Mc}) = 0 \tag{33}$$

Similarly, the governing equation for fracture solute transport can be obtained as

$$(\upsilon^F \rho_l^{Fl})\dot{c}_{Fc} - \rho_l^{Fl}\frac{k^F}{\mu_w}\nabla p^{Fl}\nabla c_{Fc} - r_{ex}^c + \nabla \cdot (\rho_l^{Fl} D^F \nabla c_{Fc}) = 0 \tag{34}$$

where $D^M$, $D^F$ are the dispersion -diffusion coefficient for the solute in porous matrix

and fracture.

The transfer term has been studied for a long time since 1960 s (Barenblatt et al., 1960, Khalili, 2003). Here a linear transfer equation is adopted, which can be described as:

$$\frac{r_{ex}^{l}}{\rho_{l}^{\alpha l}} = \frac{\chi k^{M}}{\mu_{w}}\left(p^{Ml} - p^{Fl}\right) \tag{35}$$

where the $\chi$ means shape factor, $\rho_{l}^{\alpha l}$ is the In-phase density of porous or fracture fluid. $\chi$ can be calculated as (Warren and Root, 1963)

$$\chi = \frac{4N(N+2)}{L^{2}} \tag{36}$$

where $N$ denotes the dimension of porous matrix block ( $N$ =1,2,3), $L$ is the fracture spacing.

The transfer term of the solute can be divided into two parts, convection and diffusion (Dykhuizen, 1987)

$$\frac{r_{ex}^{c}}{\rho_{l}^{\alpha l}} = \frac{\chi k^{M}}{\mu_{w}}\left(p^{Ml} - p^{Fl}\right)\left(c_{Mc} - c_{Fc}\right) + \tau\left(c_{Mc} - c_{Fc}\right) \tag{37}$$

where $\tau$ is the diffusion transfer parameter.

*Parameter identification*

The parameters in the governing equations were identified by MA et al. (2023). Below are the expressions of these parameters

$$\zeta^{F} = 1 - \frac{K}{K_{pb}} \tag{38}$$

where $K_{pb}$ denotes the bulk modulus of the porous matrix block (Valliappan and

Khalili-Naghadeh, 1990).

$$\zeta^{M} = \frac{K}{K_{pb}} - \frac{K}{K_{s}} \tag{39}$$

where $K_s$ is the bulk modulus of solid grain.

$$Z = \frac{1}{K_{pb}}\left(1-\phi^{F} - \frac{K}{K_{pb}}\right) \tag{40}$$

$$B = \left(1-\phi^{F} - \frac{K}{K_{pb}}\right)\left(\frac{1}{K_{s}} - \frac{1}{K_{pb}}\right) \tag{41}$$

$$Q = \left(\frac{1}{K_{pb}} - \frac{1}{K_{s}}\right)\left(1-\phi^{F} - \frac{K}{K_{pb}} + \frac{K}{K_{s}}\right) - \frac{\phi^{M}}{K_{s}} \tag{42}$$

These parameters can be determined directly in the laboratory test.

**Theoretical verification**

The mathematical model in the present paper (from equation (29) to (34)), obtains the effects of mechanical deformation and fluid flow on solute transport in dual-porosity media. The constitutive equation of hydro-mechanical coupling is the same as research from the mechanics approach (Khalili, 2003, Khalili, 2008b), which mainly focus on the coupling between fluid flow (including multiphase flow) and solid deformation, without exploration of the influence of hydro-mechanical coupling on solute transport. Equation (25) and (26) obtain the porosity evolution in dual-porosity media; which is determined by solid deformation, both pore and fracture pressure change. If Equation (25) and (26) are ignored, as well as the mechanical part (equation (29)), the ST-HM model can degenerate to the classical Dual-Permeability Model proposed by (Simunek

and van Genuchten, 2008).

The fluid transfer term is consistent with previous research (Khalili, 2003, Zhao and Chen, 2006). The solute transfer term is consistent with solute transport research in dual-porosity media (Dykhuizen, 1987, Li et al., 2020, Gerke and Vangenuchten, 1993). If it ignores the solute diffusion between pore and fracture, it converts to a pure convection term (Sharma et al., 2021). It converts to a pure concentration-depended term (Leij et al., 2012) if it ignores the convection between pore and fracture.

Musso and Li (Musso et al., 2013, Li et al., 2020) studied HMC coupling in swelling clay. Compared with the solute transport part in their model (i.e. ignoring swelling), the ST-HM model considers the fully coupled effects between pore and fracture fluid flow (equation (31) and (32)).

## Experimental validation of the coupled model

### *Validation strategy*

The presented model is validated by two existing laboratory tests. The first simulation is used to validate the solute transport behaviour in dual-porosity media, while the second one is used to validate the dual porosity Hydro-Mechanical coupling part.

The numerical models based on the equations proposed in this paper were used to simulate the experiments. The initial parameter's value was adopted by the experimental research, the simulated results were compared with experimental data for model validation. During the optimization, the parameters were changed to different values,

and the final optimized parameter values were obtained when the modelling results fitted well with the experimental data.

*Validation of the solute transport behaviour*

The experimental information is detailed in (Leij et al., 2012)). The details of this experiment and how the model was calibrated are provided in the supplementary material. At first, the soil column which contains both macropore and pore was saturated, and a steady flow rate of 1397.5 cm/d was established. The solute concentration ($CaCl_2$) of the inflow fluid $C_i$ was 60 mol/m$^3$. Then the concentration ($CaCl_2$) of inflow fluid $C_i$ was changed from 60 mol/m$^3$ to 90 mol/m$^{3,}$ and the concentration at each probe was measured. The relative concentration ratio $\frac{C}{C_0}$ was calculated, $C$ means the relative concentration (measured concentration minus the initial concentration 60 mol/m$^3$) and $C_0$ the concentration step (30 mol/m$^3$).

Note that the soil is dual-porosity media. So, the measured concentration was the average volumetric concentration, which was calculated as

$$C_{av} = \frac{C_{Mc} \times \upsilon^M + C_{Fc} \times \upsilon^F}{\upsilon^M + \upsilon^F} \tag{43}$$

A numerical model was set up in COMSOL Multiphysics$^{TM}$ software (AB) based on the experiment. Mechanical deformation was ignored in this simulation, and no adsorption was considered (details of the numerical model setting are provided in the supplementary materials). All simulation parameters are listed in **Table 1**.

The modelled and experimental BTC data are plotted together in **Figure 2**. The calculation error between the model results and experimental data is presented in Supplementary information.

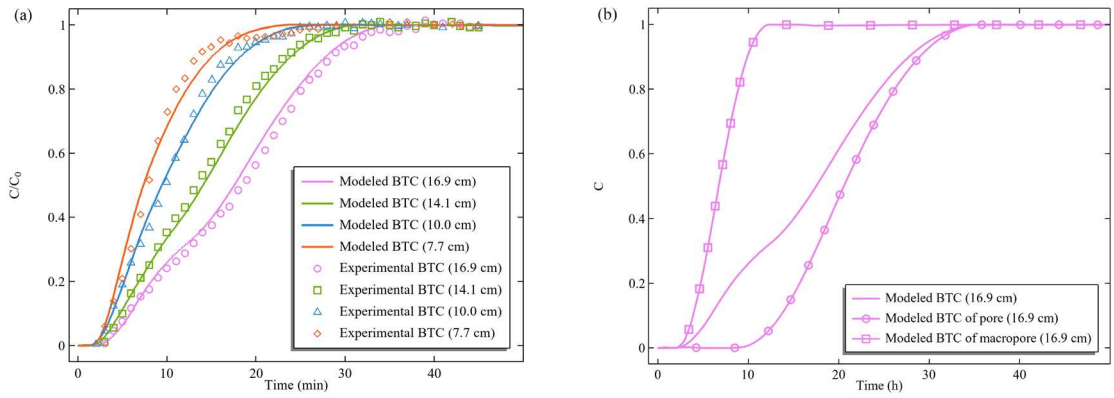


**Figure 2.** Experimental and modelled BTC at depths of 7.7, 10.0, 14.1, and 16.9 cm in (a). Modelled BTC for volume average, pore and macropore concentration at a depth of 16.9 cm in (b).

**Figure 2a** shows that the modelled results are in very close agreement with the experimental data. **Figure 2b** shows the modelled BTC of volume average, pore and macropore concentration at 16.9 cm. The peak of macropore BTC appears at about 12 h, much ahead of the peak of pore BTC (about 35 h), which leads to bimodal transport.

*Validation of hydro-mechanical coupling behaviour*

The experimental information is detailed in Callari's research (Callari and Federico, 2000). A artificial dual porosity media experienced a 1D consolidation process. Drainage of water during the consolidation was allowed through the upper boundary. The preliminary compaction was conducted under an initial effective pressure of 50 kPa; three successive load increments were applied. Here the third load increment (from

200 KPa to 400 KPa) is considered.

The details of the numerical model and how the model was calibrated are provided in the supplementary materials. All simulation parameters are listed in **Table 2**. The modelled and experimental excess fluid pressure data are plotted together in **Figure 3**. The modelled results fit well with the experimental one, except in the very early stage (less than 2 minutes). The measurement of pressure in the geotextile is quite difficult due to the high rate of pressure dissipation in the geotextile (Callari and Federico, 2000). Both modelled and experimental results show that the fluid pressures in clayey block (porous space) and geotextile (fracture space) are quite different.

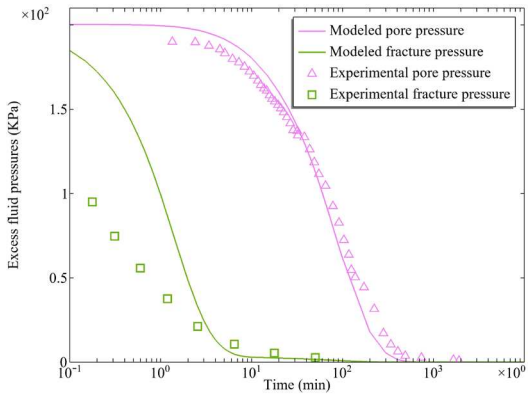


**Figure 3.** Experimental and modelled excess fluid pressure at the base of the cell versus time

## Numerical case setup

Two numerical models were set up to further illustrate the solute transport behaviour in deformable dual-porosity. The first model used the ST-HM equations, and the second used the equations in the research of Zhenze Li (Li et al., 2020), hereinafter referred to as the Zhenze model. Zhenze model deals with coupled hydro-mechanical-chemical

(HMC) behaviour in dual-porosity media, considering osmosis flow and swelling, which can interpret the swelling behaviour of MX-80 when infiltrated with brine. Osmosis flow and swelling were ignored in the presented paper, so only the non-reactive solute transport part in Zhenze model is compared with ST-HM. This comparison investigates the fully coupling effects between micropore and macropore flow on the solute transport and porosity evolution, which is not considered in Zhenze model.

As shown in **Figure 4**, the initial fluid pressure was $3\times10^6$ Pa, and the initial solute concentration was $10\,\mathrm{mol/m^3}$. The bottom boundary was a fixed constraint and no flow boundary. The overburden applies a constant vertical load of $4\times10^6$ Pa on the rock, with no flow crossing this boundary. The left boundary was constant horizontal load $2\times10^6$ Pa, and the right boundary was fixed in the X direction. In the simulation, the fluid pressure on the left boundary remained $3\times10^6$ Pa while the fluid pressure on the right boundary decreased to $1.5\times10^6$ Pa due to external human activity. The solute concentration on the left boundary changed to 60 $\mathrm{mol/m^3}$ while the concentration on the right remained at $10\,\mathrm{mol/m^3}$. The boundary conditions are referenced from (Nguyen, 2010).

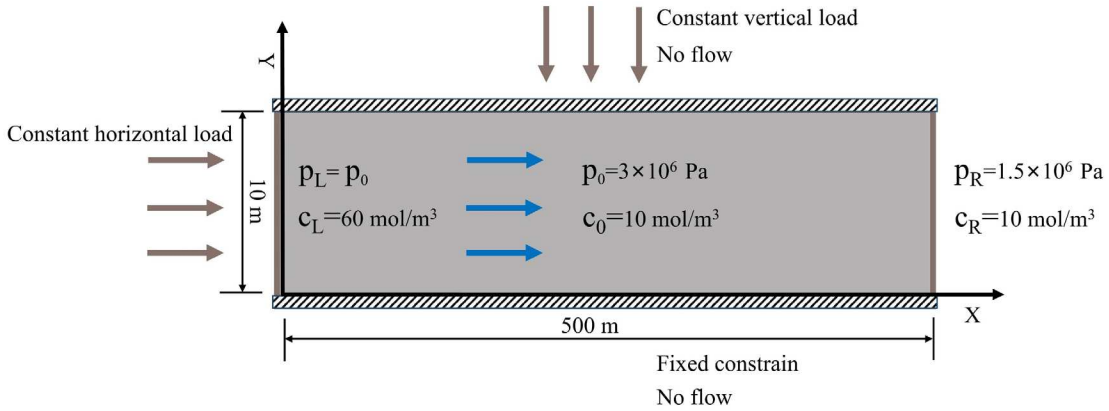


**Figure 4.** Model description and boundary conditions for an assumed aquifer

The parameters adopted in these two simulations are the same and are listed in **Table 3**. Parameters are from the research of (Gelet et al., 2012a) and (Abousleiman and Nguyen, 2005).

## Numerical case results

### *Mechanical deformation in dual-porosity media*

The effects of fluid pressure change on solid deformation are well predicted by the ST-HM model. As shown in **Figure 5**, the rock consolidates in the simulation. The displacement of the ST-HM model increases with time, finally reaching almost a steady value at about 100 d. In contrast, the displacement of Zhenze model does not change during the simulation. The reason is that fluid pressure does not influence solid deformation in Zhenze model. As the fluid pressure decreases in the rock, it leads to further consolidation until the fluid pressure reaches an equilibrium stage. Deformation is related to the evolution of fluid pressure (equation (29)), so the increased deformation rates slow with time (as the decreased rates of fluid pressure become slow).

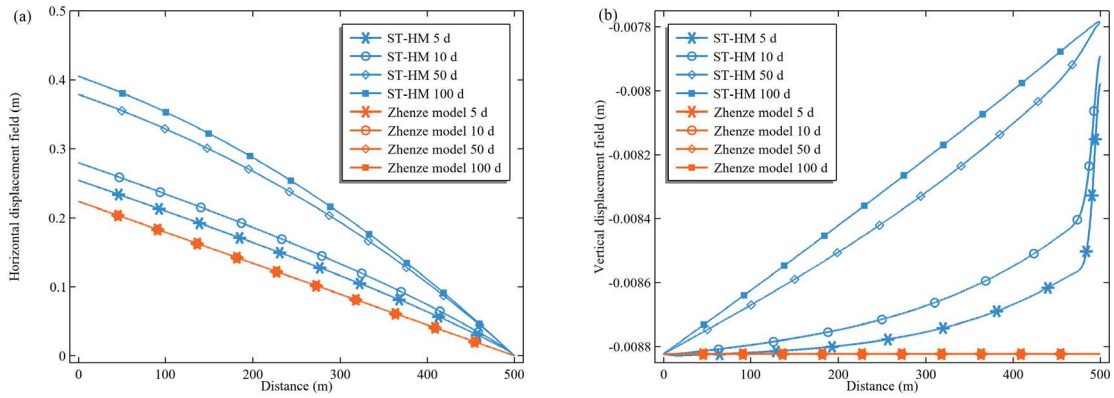


**Figure 5.** Horizontal and vertical displacement in X direction of rock

*Fluid flow coupling in dual-porosity media*

**Figure 6** shows the pressure evolution in the pore and fracture of the rock. The fluid pressure in both pores and fractures decreases gradually from the right side. Fluid pressure in fracture changes much faster than in pore due to the much higher permeability of fracture. Comparing the results of these two models, the fluid pressure of the Zhenze model in both pore and fracture decreases faster than the fluid pressure of the ST-HM model. It can be attributed to the coupled effect between pore and fracture flow which is not considered in the Zhenze model. In equation (31) and (32), the coupling term $Q\dot{p}^{Ml} + B\dot{p}^{Fl}$ in the porous fluid equation and $Z\dot{p}^{Fl} + B\dot{p}^{Ml}$ in fracture fluid equation is one of the novelties of ST-HM model. Since pore and fracture pressure decrease in the simulation domain, these two coupling terms contribute to a lower value of fluid pressure gradient (means lower water flow rates and slower decreased rates of fluid pressure) than the Zhenze model.

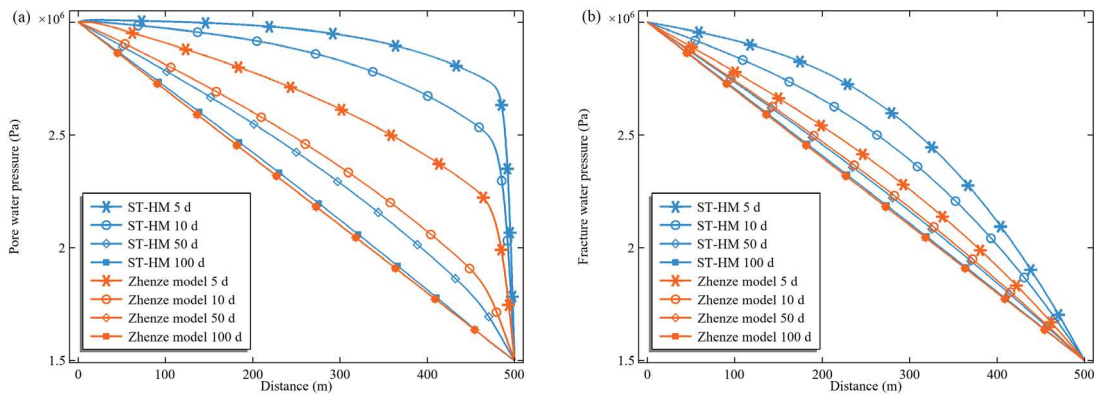


**Figure 6.** Pore and fracture fluid pressure evolution on X direction of rock

*Porosity evolution in dual-porosity media*

**Figure 7** shows the porosity evolution in pore and fracture in the X direction of rock. The pore porosity and fracture porosity all decrease in the consolidation process. However, the ST-HM model and the Zhenze model give different predictions for the evolution trend. In the the Zhenze model, porosity decreases from the initial value instantaneously and remains constant throughout the simulation because this model does not consider the influence of fluid pressure on porosity. According to equation (25) and (26), the ST-HM model considers the influence of both pore pressure and fracture pressure on porosity, so the porosity decreases gradually from the right side to the left side (as the pressure change from the right side to the left side). Compared with the Zhenze model, ST-HM model can better predict the long-term porosity change induced by fluid pressure change.

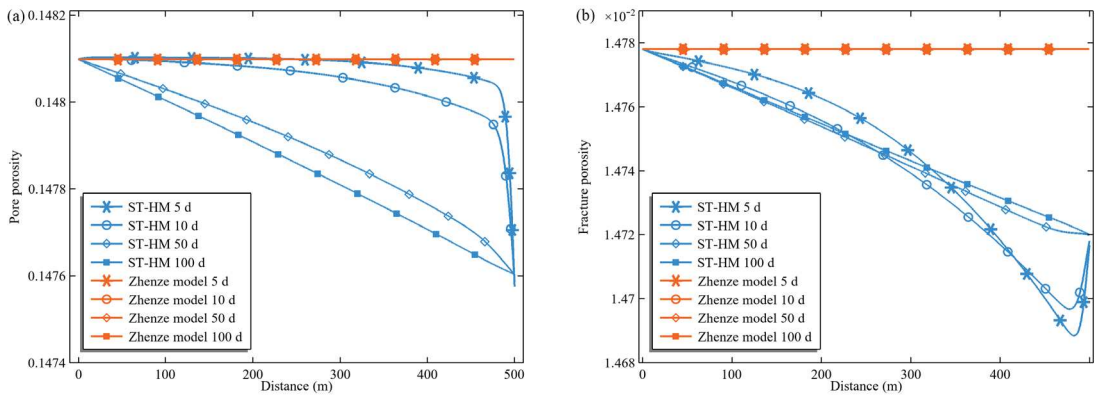


**Figure 7.** Pore and fracture porosity evolution on X direction of rock

Note that the fracture porosity at the right part reaches the lowest value in the early stage (less than 100 d) and subsequently increases to a higher value, while the left part shows the opposite trend. This can be explained based on the effects of pore pressure and fracture pressure on fracture porosity. According to equation (26), the fracture porosity is determined by solid strain, both pore and fracture pressure. In this simulation, $B = -6.65\times10^{-11}$ and $Z = 6.95\times10^{-11}$, which means that pore pressure change and fracture pressure change affect fracture porosity oppositely in this case. Between 5 to 100 days $\dot{p}^{Ml}$ is much lower than $\dot{p}^{Fl}$ at the right part of the simulation domain (because the response of fracture pressure is much quicker than pore pressure), which leads to an increase of fracture porosity at the right. While at the left part of the simulation domain, the difference of $\dot{p}^{Ml}$ and $\dot{p}^{Fl}$ is not so high to overcome the total decreased trend of fracture porosity.

The porosity change is induced by solid deformation, pore and fracture pressure. As shown in **Figure 8**, the maximum pore porosity change is about -0.0022 (accounts for 1.46% of the initial pore porosity). In comparison, the maximum fracture porosity

change is about -0.00025 (accounts for 1.67% of the initial fracture porosity). The main contribution of porosity change comes from solid deformation. Remarkably, in dual-porosity media, with the decrease of fluid pressure in both pore and fracture, the porosity responds to both pore and fracture pressure. For pore porosity, the decrease of pore pressure induces consolidation and the decrease of pore porosity. At the same time, the decrease of fracture pressure induces the expansion of pore water which increase the pore porosity. Similarly, the decrease of pore pressure induces fracture water expansion for fracture porosity, while the decrease of fracture pressure induces consolidation. As the permeability of fracture is much higher than pore, the fracture pressure reaches its equilibrium much earlier, so the influence of the pore pressure on pore and fracture porosity last longer than fracture pressure.

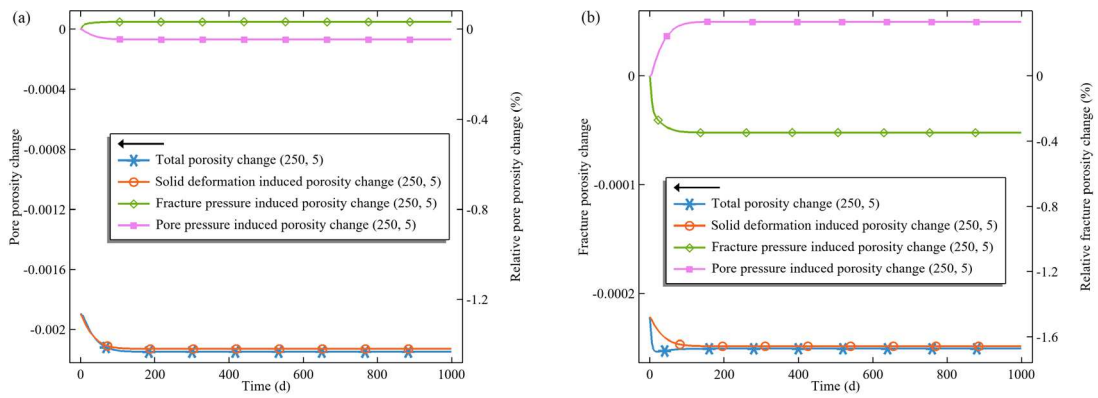


**Figure 8.** Pore and fracture porosity evolution at the centre of the rock (X=250, Y=5)

*Effects of hydro-mechanical coupling on solute transport*

The solute concentration evolution in the X direction of rock is illustrated in **Figure 9**. The solute transport is quite slow due to the low permeability of the rock. The transport

rates in the fracture are much higher than in the pore. That is, the transport in fracture dominates the transport phenomenon in this simulation. For the ST-HM model, it gives a prediction that the solute transport front reached approx. 180 m after 1000 days, while for Zhenze model this value is approx. 210 m. This difference is due to the overestimation of porosity in the Zhenze model, which also overestimates permeability and diffusivity. Hence, in most parts of the simulation domain, the concentration values predicted by Zhenze model are higher than the ST-HM model. The ST-HM model reduces about 16.67 % error for the prediction of solute transport front after 1000 days, considering the influence of fluid pressure on porosity and the coupled effect between pore and fracture flow. After 1000 days, the overestimation of fracture solute consideration is 0.41 mol/m$^3$ (accounting for 0.73 %) at 50 m, 2.85 mol/m$^3$ (accounting for 9.71 %) at 85 m, 2.26 mol/m$^3$ (accounting for 12.39 %) at 103 m. The increased rate of the difference in solute transport font location between ST-HM and Zhenze model becomes slow with time (because the pressure gradient and concentration gradient decrease throughout the simulation).

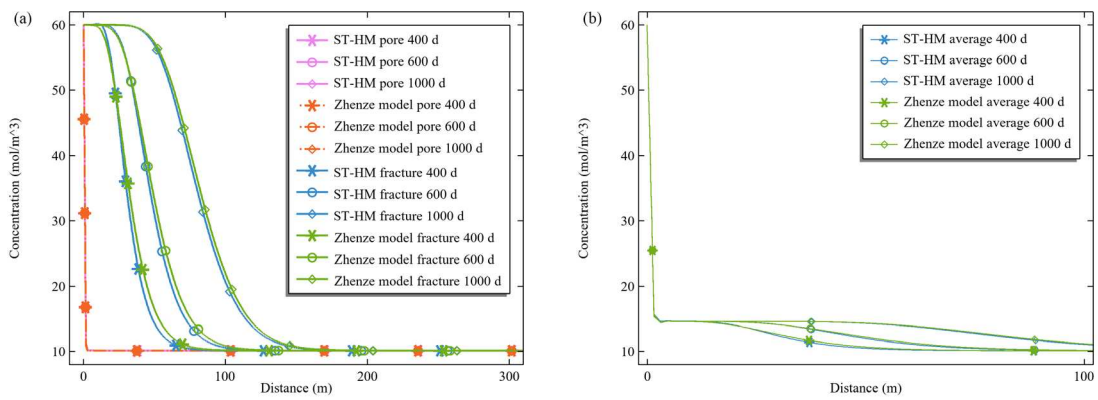


**Figure 9.** Solute concentration evolution on the X direction of rock (fracture

concentration, pore concentration and average volumetric concentration)

**Discussion of advantages and limitations**

This study presents a novel method based on nonequilibrium thermodynamics rather than the traditional mechanics approach. Since it is an energy-based approach, it is easy to bridge different behaviour and extendable for other processes such as thermo-hydro-mechanical-chemical and bio-hydro-mechanical-chemical coupling.

The governing equation in this paper is based on the assumption of small deformation and isotropic, these equations for hydro and mechanical fields are similar to research from the mechanics approach (Khalili, 2003, Khalili, 2008b). If these assumptions are released, more general governing equations are likely to be obtained, which shows an advantage of mixture-coupling theory over the classical mechanics approach on deriving complicated multi-physics in a systematic way.

The consideration of hydro-mechanical coupling on solute transport in dual-porosity media is an advancement to the classical Dual-Permeability Model proposed by Simunek and van Genuchten (2008). This model captures the fully coupling effects of pore and fracture flow with mechanical deformation. By engaging this effect, the solid stress and the porosity change can be better predicted than the classical model. Since ignoring the fully coupling effects of pore and fracture fluid can induce significant error, especially for long-term prediction, the ST-HM model can significantly reduce the error for the prediction of the solute transport front compared with the equations by Li et al. (2020).

There are also some limitations existed in this model. The potential effects of exchange on the transport phenomenon in pore and fracture were not studied. In addition, high-velocity flow would affect the dissipation process in porous media (Takhanov, 2011). So, the modification of general Darcy's law in dual-porosity media is needed to implement these limitations.

Finally, the basic assumption of the dual-porosity theory is that the different spaces in the media and the exchange phenomenon between those spaces can be captured by the equivalent continuous parameters and variables (Berre et al., 2019). The proposed model is not capable to solve solute transport in some fractured or structured media with insignificant dual porosity characteristics.

## Conclusion

This research extends the Mixture Coupling Theory and derives the constitutive equations for non-reactive solute transport in deformable dual-porosity media (ST-HM), based on nonequilibrium thermodynamics. The final governing equations of ST-HM enable the prediction of non-reactive solute transport considering fully hydro-mechanical coupling, which was often ignored by existing research.

A conceptual case was simulated to illustrate the major improvement of the presented model. Simulated results show that the presented model provides a better prediction than a previous model on the porosity evolution, fluid pressure and solute concentration due to the consideration of fully coupling effects between pore and fracture flow. The ST-HM model reduces about 16.67 % error for the prediction of solute transport front

after 1000 days and reduces up to 12.39 % error for the prediction of fracture concentration.

**Acknowledgement**

The first, second, third, and sixth authors would like to thank the National Key R&D Program of China (No.2019YFC1805503). The first and sixth authors would like to thank the National Key R&D Program of China (No.2018YFC1800905) and the Key science and technology projects of Inner Mongolia autonomous region (2019ZD001). The fourth author would like to thank the CERES studentship support from the School of Civil Engineering at the University of Leeds. All the authors would like to thank Dr Shashank Bettadapura Subramanyam for his help with the language editing of this paper.

# Reference


Ab, C. *COMSOL Multiphysics®*, Stockholm, Sweden., See www.comsol.com.

Abousleiman, Y. & Nguyen, V. (2005) Poromechanics Response of Inclined Wellbore Geometry in Fractured Porous Media. *Journal of Engineering Mechanics-asce - J ENG MECH-ASCE* **131**.

Akono, A.-T., Druhan, J. L., Davila, G., Tsotsis, T., Jessen, K., Fuchs, S., Crandall, D., Shi, Z., Dalton, L., Tkach, M. K., Goodman, A. L., Frailey, S. & Werth, C. J. (2019) A review of geochemical-mechanical impacts in geological carbon storage reservoirs. *Greenhouse Gases-Science and Technology* **9(3)**:474-504.

Arson, C. & Pereira, J. M. (2013) Influence of damage on pore size distribution and permeability of rocks. *International Journal for Numerical and Analytical Methods in Geomechanics* **37(8)**:810-831.

Barenblatt, G. I., Zheltov, I. P. & Kochina, I. N. (1960) Basic concepts in the theory of seepage of homogeneous liquids in fissured rocks [strata]. *Journal of Applied Mathematics and Mechanics* **24(5)**:1286-1303.

Bedford, A. & Drumheller, D. S. (1983) Theories of Immiscible and Structured Mixtures. *International Journal of Engineering Science* **21(8)**:863-960.

Berre, I., Doster, F. & Keilegavlen, E. (2019) Flow in Fractured Porous Media: A Review of Conceptual Models and Discretization Approaches. *Transport in Porous Media* **130(1)**:215-236.

Biot, M. A. (1941) General theory of three-dimensional consolidation. *Journal of Applied Physics* **12(2)**:155-164.

Bitzer, K. (1996) Modeling consolidation and fluid flow in sedimentary basins. *Computers & Geosciences* **22(5)**:467-478.

Bowen, R. M. (1976) Theory of Mixtures. *Continuum Physics*:1-127.

Bowen, R. M. (1984) Porous Media Model Formulations by the Theory of Mixtures. *Fundamentals of Transport Phenomena in Porous Media*.

Brochard, L. & Honório, T. (2020) Revisiting thermo-poro-mechanics under adsorption: Formulation without assuming Gibbs-Duhem equation. *International Journal of Engineering Science* **152**:103296.

Callari, C. & Federico, F. (2000) Fem validation of a double porosity elastic model for consolidation of structurally complex clayey soils. *International Journal for Numerical and Analytical Methods in Geomechanics* **24(4)**:367-402.

Chen, X. (2013) Constitutive unsaturated hydro-mechanical model based on modified mixture theory with consideration of hydration swelling. *International Journal of Solids and Structures* **50(20-21)**:3266-3273.

Chen, X. & Hicks, M. A. (2011) A constitutive model based on modified mixture theory for unsaturated rocks. *Computers and Geotechnics* **38(8)**:925-933.

Chen, X. & Hicks, M. A. (2013) Unsaturated hydro-mechanical-chemo coupled constitutive model with consideration of osmotic flow. *Computers and Geotechnics* **54**:94-103.

Chen, X., Pao, W., Thornton, S. & Small, J. (2016) Unsaturated hydro-mechanical-chemical constitutive coupled model based on mixture coupling theory: Hydration swelling and chemical osmosis. *International Journal of Engineering Science* **104**:97-109.

Coussy, O. (2004) *Poromechanics.* England, John Wiley & Sons Inc.

De Bellis, M. L., Della Vecchia, G., Ortiz, M. & Pandolfi, A. (2016) A linearized porous brittle damage material model with distributed frictional-cohesive faults. *Engineering Geology* **215**:10-24.

De Bellis, M. L., Della Vecchia, G., Ortiz, M. & Pandolfi, A. (2017) A multiscale model of distributed fracture and permeability in solids in all-round compression. *Journal of the Mechanics and Physics of Solids* **104**:12-31.

Drumheller, D. S. (1978) The theoretical treatment of a porous solid using a mixture theory. *International Journal of Solids & Structures* **14(6)**:441-456.

Duguid, J. O. & Lee, P. C. Y. (1977) Flow in fractured porous media. *Water Resources Research* **13(3)**:558-566.

Dykhuizen, R. C. (1987) Transport of solutes through unsaturated fractured media. *Water Research* **21(12)**:1531-1539.

Dykhuizen, R. C. (1990) A new coupling term for dual-porosity models. *Water Resources Research* **26(2)**:351-356.

Gelet, R., Loret, B. & Khalili, N. (2012a) Borehole stability analysis in a thermoporoelastic dual-porosity medium. *International Journal of Rock Mechanics and Mining Sciences* **50**:65-76.

Gelet, R., Loret, B. & Khalili, N. (2012b) A thermo-hydro-mechanical coupled model in local thermal non-equilibrium for fractured HDR reservoir with double porosity. *Journal of Geophysical Research: Solid Earth* **117(B7)**.

Gerke, H. H. & Vangenuchten, M. T. (1993) A dual-porosity model for simulating the preferential movement of water and solutes in structured porous-media. *Water Resources Research* **29(2)**:305-319.

Heidug, W. K. & Wong, S. W. (1996) Hydration swelling of water-absorbing rocks: a constitutive model. *International Journal for Numerical and Analytical Methods in Geomechanics* **20(6)**:403-430.

Hutter, K., Laloui, L. & Vulliet, L. (2015) Thermodynamically based mixture models of saturated and unsaturated soils. *International Journal for Numerical & Analytical Methods in Geomechanics* **4(4)**:295-338.

Jiang, J. & Younis, R. M. (2017) An Improved Projection-based Embedded Discrete Fracture Model (pEDFM) for Multiphase Flow in Fractured Reservoirs. *Advances in Water Resources* **109**.

Khalili, N. (2003) Coupling effects in double porosity media with deformable matrix. *Geophysical Research Letters* **30(22)**.

Khalili, N. (2008a) Two-phase fluid flow through fractured porous media with deformable matrix. *Water Resources Research* **44(5)**.

Khalili, N. (2008b) Two-phase fluid flow through fractured porous media with deformable matrix: TWO-PHASE FLUID FLOW THROUGH FRACTURED POROUS MEDIA. *Water Resources Research* **44(5)**.

Kodešova, R., Šimůnek Josef, K. & Jiři (2006) Numerical Study of Macropore Impact on Ponded Infiltration in Clay Soils. *Soil and Water Research* **1(1)**:16-22.

Laloui, L., Klubertanz, G. & Vulliet, L. (2003) Solid-liquid-air coupling in multiphase porous media. *International Journal for Numerical and Analytical Methods in Geomechanics* **27(3)**:183-206.

Lee, S. H., Lough, M. F. & Jensen, C. L. (2001) Hierarchical modeling of flow in naturally fractured formations with multiple length scales. *Water Resources Research* **37(3)**:443–455.

Leij, F. J., Toride, N., Field, M. S. & Sciortino, A. (2012) Solute transport in dual-permeability porous media. *Water Resources Research* **48**.

Li, Z., Su, G., Zheng, Q. & Nguyen, T. S. (2020) A dual-porosity model for the study of chemical effects on the swelling behaviour of MX-80 bentonite. *Acta Geotechnica* **15(3)**:635-653.

Liu, J., Wang, J. G., Gao, F., Leung, C. F. & Ma, Z. (2019) A fully coupled fracture equivalent continuum-dual porosity model for hydro-mechanical process in fractured shale gas reservoirs. *Computers and Geotechnics* **106**:143-160.

Ma, Y., Chen, X.-H., Hosking, L. J., Yu, H.-S., Thomas, H. R. & Norris, S. (2021) The influence of coupled physical swelling and chemical reactions on deformable geomaterials. *International Journal for Numerical and Analytical Methods in Geomechanics* **45(1)**:64-82.

Ma, Y., Feng, J., Ge, S., Wang, K., Chen, X. & Ding, A. (2023) Constitutive modelling of Hydro-Mechanical coupling in double porosity media based on Mixture Coupling Theory. *International Journal of Geomechanics*.

Molson, J., Aubertin, M. & Bussiere, B. (2012) Reactive transport modelling of acid mine drainage within discretely fractured porous media: Plume evolution from a surface source zone. *Environmental Modelling & Software* **38**:259-270.

Murad, M. A. & Moyne, C. (2008) A dual-porosity model for ionic solute transport in expansive clays. *Computational Geosciences* **12(1)**:47-82.

Musso, G., Romero, E. & Della Vecchia, G. (2013) Double-structure effects on the chemo-hydro-mechanical behaviour of a compacted active clay. *Geotechnique* **63(3)**:206-220.

Nguyen, V. X. (2010) Dual-porosity and dual-permeability poromechanics solutions for problems in laboratory and field applications.) OK: The University of Oklahoma, Ann Arbor.

Oda, M. (1985) PERMEABILITY TENSOR FOR DISCONTINUOUS ROCK MASSES. *Geotechnique* **35(4)**:483-495.

Rajagopal & K., R. (2007) On a hierarchy of approximate models for flows of incompressible fluids through porous solids. *Mathematical Models and Methods in Applied Sciences* **17(02)**:215-252.

Ray, C. (1994) Modeling transport of agricultural chemicals in a dual porosity system resulting from macropores.) IL: University of Illinois at Urbana-Champaign, Ann Arbor, pp. 159.

Revil, A. (2017) Transport of water and ions in partially water-saturated porous media. Part 2. Filtration effects. *Advances in Water Resources* **103**:139-152.

Rutqvist, J. & Stephansson, O. (2003) The role of hydromechanical coupling in fractured rock engineering. *Hydrogeology Journal* **11(1)**:7-40.

Saevik, P. N., Berre, I., Jakobsen, M. & Lien, M. (2013) A 3D Computational Study of Effective Medium Methods Applied to Fractured Media. *Transport in Porous Media* **100(1)**:115-142.

Savatorova, V. L., Talonov, A. V. & Vlasov, A. N. (2016) Upscaling of dual-porosity models for gas transport in organic-rich shales. *Composites-Mechanics Computations Applications* **7(3)**:233-259.

Sharma, A., Swami, D., Joshi, N., Chandel, A. & Simunek, J. (2021) The Semi-Analytical Solution for Non-Equilibrium Solute Transport in Dual-Permeability Porous Media. *Water Resources Research* **57(5)**.

Shu, Z. (1999) A dual-porosity model for two-phase flow in deforming porous media.) OK: The University of Oklahoma, Ann Arbor, pp. 185.

Simunek, J. & Van Genuchten, M. T. (2008) Modeling nonequilibrium flow and transport processes using HYDRUS. *Vadose Zone Journal* **7(2)**:782-797.

Takhanov, D. (2011) Forchheimer model for non-Darcy flow in porous media and fractures.

Terzaghi, K. (1943) Theory of Consolidation. In *Theoretical Soil Mechanics*.) John Wiley & Sons, Inc, NewYork, pp. 265-296.

Valliappan, S. & Khalili-Naghadeh, N. (1990) Flow through fissured porous media with deformable matrix. *International Journal for Numerical Methods in Engineering* **29(5)**:1079-1094.

Vecchia, G. D. & Musso, G. (2016) Some remarks on single- and double-porosity modeling of coupled chemo-hydro-mechanical processes in clays. *Soils and Foundations -Tokyo-* **56(5)**:779-789.

Warren, J. E. & Root, P. J. (1963) The behavior of naturally fractured reservoirs. *Society of Petroleum Engineers Journal* **3(3)**:245-255.

Zhao, Y. & Chen, M. (2006) Fully coupled dual-porosity model for anisotropic formations. *International Journal of Rock Mechanics and Mining Sciences* **43(7)**:1128-1133.

**Table 1** *Parameters used in the numerical model against solute transport experiment*

| Parameter | Value | Meaning |
|---|---|---|
| $\rho$ | $8.5\times10^{2}$ kg·m$^{-3}$ | bulk density of Andisol |
| $\mu_w$ | $8\times10^{-4}$ Pa·s | Viscosity of water |
| $\upsilon^M$ | 0.41 | Initial pore porosity |
| $\upsilon^F$ | 0.16 | Initial macro pore porosity |
| $k^M$ | $2.75\times10^{-9}$ m$^2$ | Initial pore permeability |
| $k^F$ | $8.5\times10^{-9}$ m$^2$ | Initial macro pore permeability |
| $K_w$ | 4.3 GPa | Compressibility of water |
| $L$ | $1\times10^{-2}$ m | Macro pore spacing |
| $D^M$ | $7\times10^{-5}$ m$^2$·s$^{-1}$ | Pore Hydrodynamic dispersion coefficient |
| $D^F$ | $2.5\times10^{-4}$ m$^2$·s$^{-1}$ | Macro pore Hydrodynamic dispersion coefficient |
| $\tau$ | $1\times10^{-8}$ s$^{-1}$ | Coefficient of diffusive transfer |
| T | 70 min | Calculation period |
| Step | 0.1 min | Timestep |

**Table 2** *Parameters used in the numerical model against hydro-mechanical coupling experiment*

| Parameter | Value | Meaning |
|---|---|---|
| $\rho$ | $2.5\times10^{3}$ kg·m$^{-3}$ | bulk density of soil |
| $\mu_w$ | $8\times10^{-4}$ Pa·s | Viscosity of water |
| $\nu$ | 0.3 | Poisson's ratio |
| $K$ | 3.2 MPa | Bulk modulus of total rock |
| $K_{Pb}$ | 6.6 MPa | Bulk modulus of porous block |
| $K_s$ | 27.5 GPa | Bulk modulus of solid grain |
| $\upsilon^M$ | 0.55 | Initial pore porosity |
| $\upsilon^F$ | 0.008 | Initial fracture porosity |

| | | |
|---|---|---|
| $k^M$ | $4.8\times10^{-18}$ m$^2$ | Initial pore permeability |
| $k^F$ | $4\times10^{-11}$ m$^2$ | Initial fracture permeability |
| $K_w$ | 4.3 GPa | Compressibility of water |
| $L$ | $6\times10^{-3}$ m | Fracture spacing |
| T | $10^4$ min | Calculation period |
| Step | 0.01 min | Timestep |

**Table 3** *Parameters used in the numerical simulation for discussion of solute transport behaviour in deformable dual-porosity*

| Parameter | Value | Meaning |
|---|---|---|
| $K$ | 1.103 GPa | Bulk modulus of rock |
| $K_{Pb}$ | 1.226 GPa | Bulk modulus of porous block |
| $K_s$ | 27.5 GPa | Bulk modulus of solid grain |
| $\nu$ | 0.22 | Poisson's ratio |
| $\mu_w$ | $8\times10^{-4}$ Pa·s | Viscosity of water |
| $\upsilon^M$ | 0.15 | Initial pore porosity |
| $\upsilon^F$ | 0.015 | Initial fracture porosity |
| $k^M$ | $5\times10^{-18}$ m$^2$ | Initial pore permeability |
| $k^F$ | $5\times10^{-15}$ m$^2$ | Initial fracture permeability |
| $K_w$ | 4.3 GPa | Compressibility of water |
| $D^M$ | $9\times10^{-12}$ m$^2$·s$^{-1}$ | Pore Hydrodynamic dispersion coefficient |
| $D^F$ | $7\times10^{-11}$ m$^2$·s$^{-1}$ | Fracture Hydrodynamic dispersion coefficient |
| $\tau$ | $1\times10^{-11}$ s$^{-1}$ | Coefficient of diffusive transfer |
| $L$ | 2 m | Fracture spacing |
| T | 1000 d | Calculation period |
| Step | 0.1 d | Timestep |

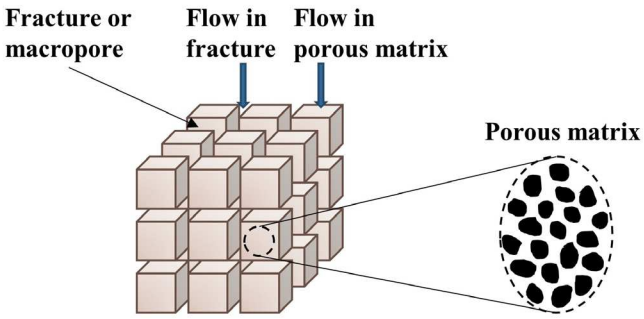


**Figure 1.** Conceptual description of the dual-porosity theory

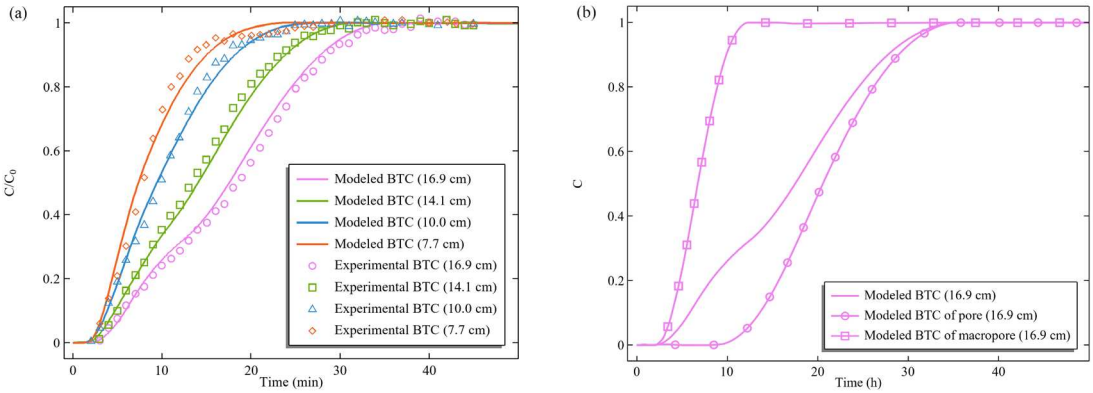


**Figure 2.** Experimental and modelled BTC at depths of 7.7, 10.0, 14.1, and 16.9 cm in (a). Modelled BTC for volume average, pore and macropore concentration at depth 16.9 cm in (b).

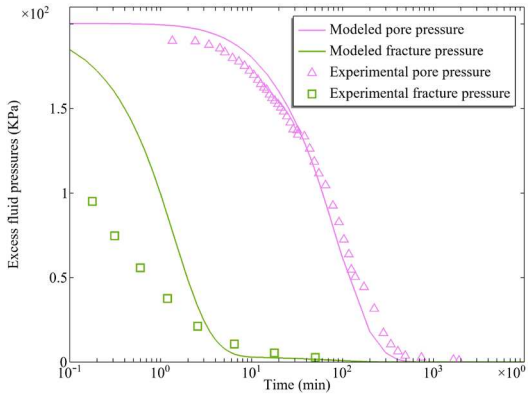


**Figure 3.** Experimental and modelled excess fluid pressure at the base of the cell versus time

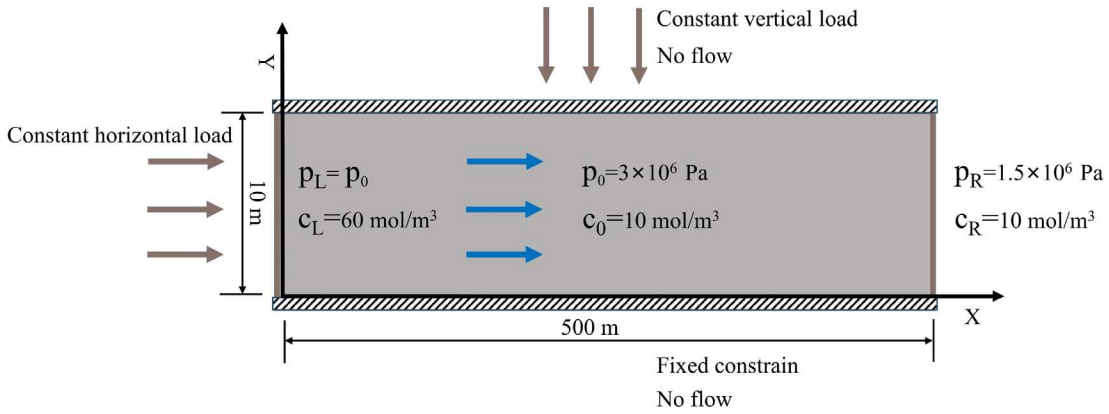


**Figure 4.** Model description and boundary conditions for an assumed aquifer

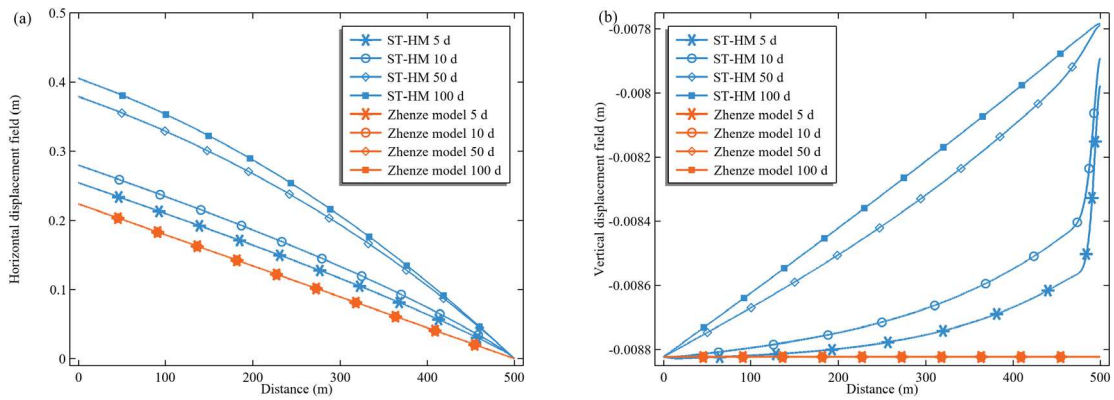


**Figure 5.** Horizontal and vertical displacement on X direction of rock

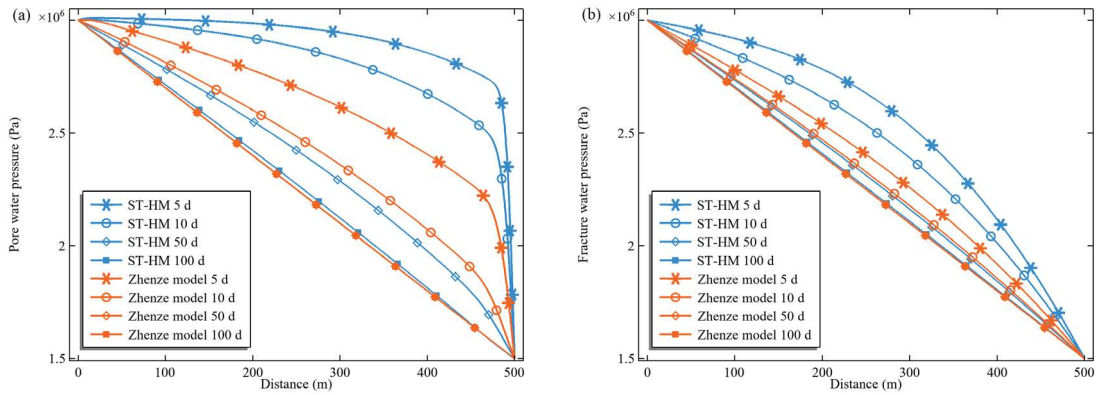


**Figure 6.** Pore and fracture fluid pressure evolution on X direction of rock

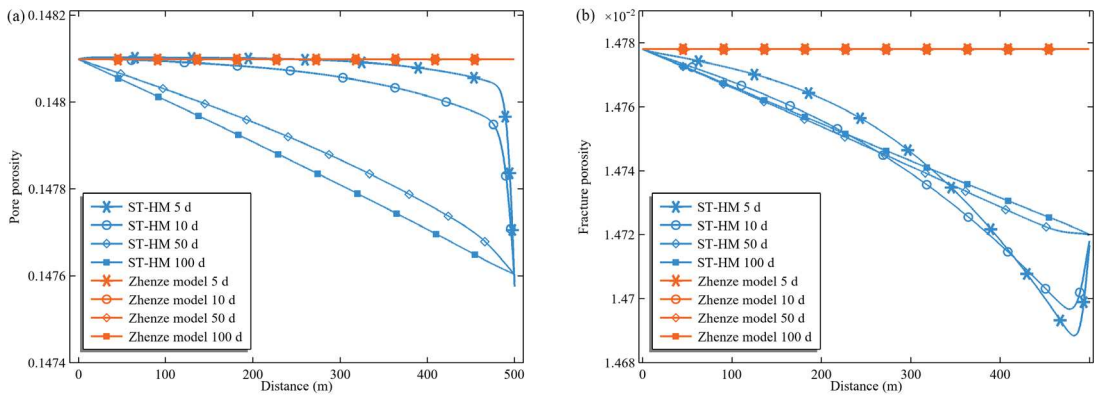


**Figure 7.** Pore and fracture porosity evolution on X direction of rock

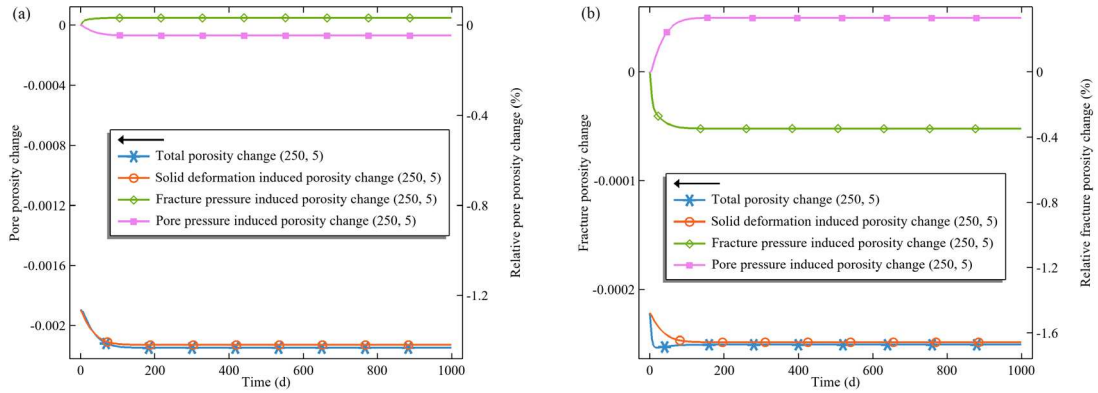


**Figure 8.** Pore and fracture porosity evolution at centre of the rock (X=250, Y=5)

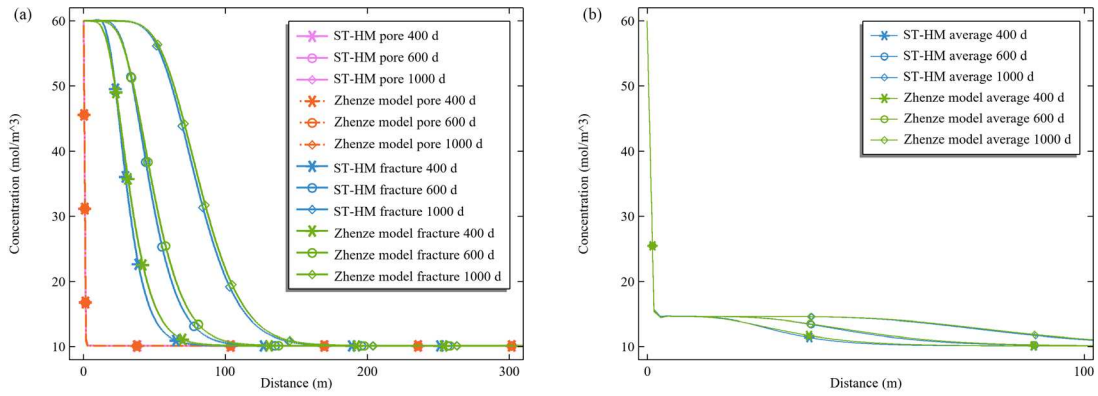


**Figure 9.** Solute concentration evolution on the X direction of rock (fracture concentration, pore concentration and average volumetric concentration)